Adaptive acoustic imaging using aberration correction in difficult materials

S D Sharples, M Clark, I J Collison and M G Somekh

Paper presented at NDT 2004, the 43rd Annual British Conference on NDT, September 2004, Torquay, UK.

This paper describes the key technological developments in the design of an adaptive optical scanning acoustic microscope. Adaption is a key technological advance because it enables the microscope to correct for the deleterious effects of the material microstructure, and gain robust instrument performance on a wide range of samples. The two important requirements for the instrument are a multi-channel acoustic wavefront detector to measure the aberration in the acoustic wavefront, and a highly adaptive acoustic source to correct for the effects of aberration. As well as describing the novel aspects of the instrument that allow it to adapt, we present experimental surface acoustic wave images acquired by the instrument that indicate the degree of performance improvement that can be achieved when adaption is used to correct for material aberration.

1. Introduction

A wavefront propagating through an aberrating medium is distorted as it travels. Typical engineering materials such as metals aberrate ultrasound propagating through them because they are made up of many grains of random orientation. The velocity of the ultrasound depends on the grain orientation, and so different parts of the wavefront travel at different velocities – this leads to distortion. The effects that this has on ultrasonic measurements include signal drop-out, high variability in velocity and amplitude measurements, a reduction in the highest usable frequency (corresponding to a reduction in the highest attainable resolution), reduced probability of detection (PoD), and poor quality, blotchy C-scan images. Aberration due to velocity variability should not be confused with the effects of scattering – which leads to attenuation and reduced resolution – because the propagating ultrasonic wavefront is distorted rather than scattered. In many cases the effects of aberration, rather than scattering, affect an instrument's upper resolution or maximum propagation distance. An analogy is the effect of the Earth's atmosphere on the light from distant stars. These 'twinkle' because the optical wavefront is distorted by the moving atmosphere. With a relatively well-known technique it is possible to correct for the atmospheric effects by actively changing the shape of a telescope mirror[1].

For a number of years we have been developing an adaptive all-optical scanning acoustic microscope (O-SAM) that would be able to detect and correct for the effects of material microstructure in order to improve measurement quality and reliability, and improve performance in terms of resolution and the range of materials on which measurements can be performed. Although the instrument is relatively specialised – it uses lasers to generate and detect surface acoustic waves – the techniques employed and knowledge gained are directly applicable to more traditional ultrasonic NDT tests, especially those employing phased arrays, testing of highly aberrating materials, and tests involving propagating over relatively long distances or at high frequencies.

The O-SAM instrument has been described previously[2, 3], and is capable of rapid, high resolution, non-destructive vector contrast imaging of surface acoustic waves (SAWs) without any measurement perturbation, damage or contamination of the sample surface. Light from a reasonably high-powered Q-switched mode locked laser – fundamental frequency 82 MHz, with harmonics extending beyond 1 GHz – is imaged onto the surface of a material, typically in the form of a concentric set of arcs, spaced to match the wavelength of the acoustic waves on the material. In the case of isotropic materials, these acoustic waves propagate to a diffraction-limited focus, where their amplitude and phase is measured by another laser, previously using a simple modified knife-edge detection technique. It is this knife-edge detector that has recently been replaced by a custom acoustic wavefront sensor (AWFS), and it is the integration of this device into the O-SAM system in order to 'close the loop' of aberration detection and correction that is the main topic of this paper.

2. Effects of material aberrations

Figure 1 illustrates schematically and experimentally the effect that material anisotropy has on the propagation of focused acoustic waves.

The upper images in the Figure illustrate the propagation of focused SAWs on an isotropic medium – the upper right-hand image shows an aerial point spread function (PSF) taken on aluminium-coated glass at 82 MHz. This image was acquired

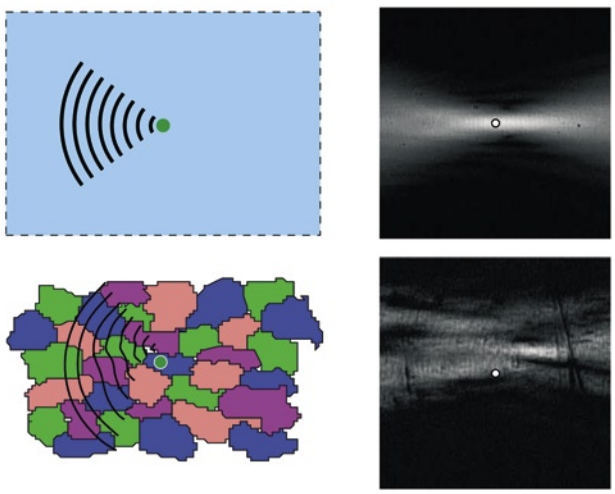

Figure 1. The upper images illustrate the propagation of SAWs on an isotropic medium – the upper right-hand image is an aerial PSF taken on aluminium-coated glass. The lower images illustrate the propagation of focused SAWs on a multi-grained anisotropic medium – the lower right-hand image is an aerial PSF taken on aluminium

The authors are at the School of Electrical & Electronic Engineering, University of Nottingham, University Park, Nottingham, NG7 2RD, UK. Tel: +44 (0)115 9515556; Fax: +44 (0)115 9515616; E-mail: steve.sharples@nottingham.ac.uk

with the O-SAM instrument by fixing the relative positions of the sample and the excitation profile, and raster-scanning the detection point. The location of the intended SAW detection point is also marked in the Figure. The lower images of Figure 1 illustrate the propagation of focused SAWs on a multi-grained anisotropic medium – the lower right-hand image is an aerial PSF taken on aluminium. Not only does the majority of the acoustic energy miss the geometric focus of the excitation arcs, but the PSF has clearly broadened and dispersed.

In its normal mode of operation, the O-SAM acquires SAW C-scan images by detecting the surface waves at the acoustic focus – fixing the relative positions of the excitation source and the detection point – and raster-scanning the material. Material anisotropy affects the quality of the images obtained[3, 4] because the acoustic energy is no longer focused to the detection point. This has important implications in non-destructive testing applications, where the acoustic energy is not probing the intended parts of the material. The 'signal drop-out' does not occur due to attenuation or scattering, rather because the acoustic energy has been displaced.

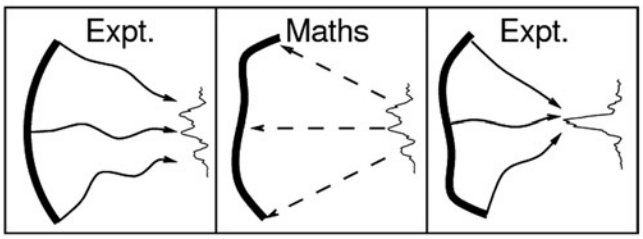

Figure 2. The Figure illustrates schematically the process of higher order wavefront correction. The aberrated wavefront is acquired in the left-hand part of the Figure. This is back-propagated to the excitation region (centre) and the difference between this and the geometrical ideal is then used as the excitation pattern (right-hand side)

3. Correcting for the effects of aberrations

To correct for the effects of material aberrations we require knowledge of the effects of the aberrations, and a method of adjusting the excitation profile to correct for them. The principle is illustrated in Figure 2.

In the case of the O-SAM instrument, we use a spatial light modulator (SLM) to achieve the excitation profile adjustment[3]. We have previously shown that if it is possible to acquire the complex amplitude of the PSF on the plane perpendicular to the propagation direction at the desired point of detection, then it is possible to use this information to generate a new excitation profile to redirect the acoustic waves back to the detection point. In the case of weakly aberrating materials, this may be achieved by simply 'tilting' the arc excitation profile, to steer the acoustic energy back to its intended destination[3]. A higher-order correction technique[5] is required to correct for aberrations that break up the wavefront as well as displacing it. This technique involves the back-propagation of the measured acoustic field using an angular spectrum propagation technique[6], where the phase error is calculated compared to the geometric excitation profile. This error is then used to generate a new excitation profile.

In both cases shown previously, the wavefront information was acquired by scanning a single-point detector across the acoustic focus using a mechanical stage. This needs to be done for each point in a C-scan image (although there is obviously a certain degree of correlation between nearby points) and adds a significant overhead to the data acquisition time. It was shown in[5] that 16 discrete points along the PSF was sufficient – even with poor signal-to-noise ratios – to achieve successful higher order correction.

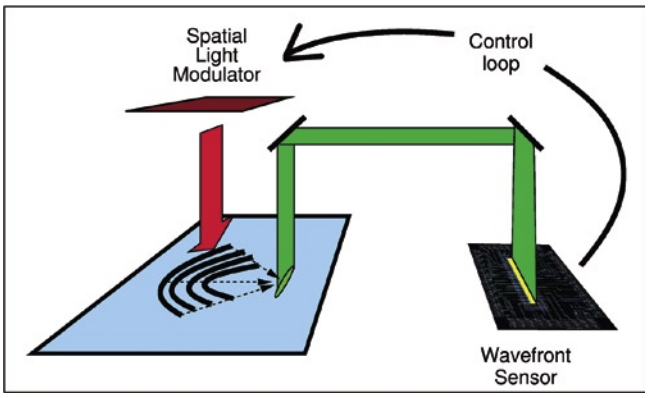

Figure 3. Schematic of the all-optical scanning acoustic microscope, employing a spatial light modulator to control the SAW excitation profile, and an acoustic wavefront sensor to acquire information about the SAWs as they propagate

4. The Acoustic Wavefront Sensor (AWFS)

At the heart of the acoustic wavefront sensor developed is a 16 x 2 array of photodetectors, designed and constructed using a standard 0.7 µm CMOS process. The pitch of the array is 100 µm per pixel. Although the full bandwidth of the device has not yet been ascertained, it is capable of detecting acoustic waves at a frequency

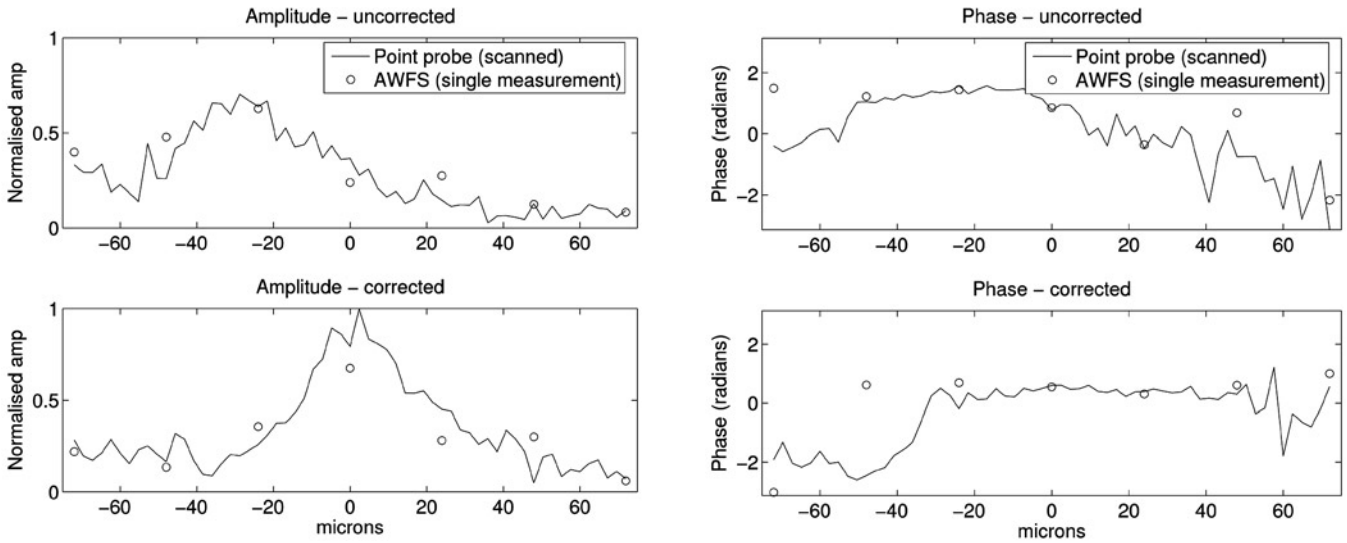

Figure 4. PSFs acquired by mechanically scanning a single-point detector (solid line) and in a single measurement using the AWFS (o). The data from just seven points acquired by the AWFS in the upper plots is enough to correct for the aberrations, as shown by the increased amplitude and correct location of the central peak in the lower amplitude plot

of 328 MHz[7]. Each pair of photodiodes in the 16 x 2 array measures the angular displacement of a focused beam reflected from the sample surface, as it is perturbed by the surface acoustic waves. Its place within the O-SAM instrument is illustrated schematically in Figure 3.

A green laser is focused onto the sample at the acoustic focus using a standard lens. A slight astigmatism is added by the addition of a weak cylindrical lens, to produce a line approximately 200 µm long on the sample surface that is diffraction limited in the orthogonal direction – the direction of SAW propagation. This line is then imaged onto the AWFS using another set of lenses. As different parts of the line on the sample are perturbed by the acoustic wavefront, the perturbations are detected by elements of the 16 channel array according to their position.

5. Results

At this early stage of integration of the AWFS into the O-SAM, only seven of the 16 elements are used. This allows us to illustrate proof of concept and demonstrate the robustness of the correction algorithm, given the relatively small amount of data from the AWFS. It should be stressed that there is absolutely no technological or systematic difficulty in adding more channels to the system - due to its highly modular design – it is simply a case of populating a couple more circuit boards.

Figure 4 illustrates the kind of data the AWFS acquires, for each point on a C-scan, both before (upper plots) and after (lower plots) correction. The continuous line is a measured point spread function acquired by mechanically scanning a single-point detector, and the circles represent the data taken by the AWFS in a single measurement. Although the data from the AWFS is much more sparse, the data from the mere seven marked points on the upper plots provide enough information for the correction algorithm to successfully perform aberration correction. The AWFS is several orders of magnitude faster, and is limited by the repetition rate of the excitation laser (several kHz) rather than the mechanical scanning speed.

Figure 5 illustrates the improvement in data quality that can be achieved using aberration correction. The images are acoustic amplitude and phase C-scans at 82 MHz on a piece of aluminium. There are no defects (apart from some superficial scratches) on the material, and in these circumstances it would be expected that uniform amplitude and phase images should be observed. Material microstructure has caused acoustic aberration however, and the effects of this are illustrated in the upper images. After aberration correction – performed by measuring the acoustic wavefront at each detection point and then customising the SAW excitation profile to accommodate the material microstructure – significantly more uniform amplitude and phase images are acquired (lower images.)

6. Conclusions

The results presented are, as stated, early results from a system in the first stages of integration and development. Nevertheless they illustrate that simultaneous detection of a SAW wavefront at several discrete points is possible with an acoustic wavefront sensor, and that this information can be used to correct for the effects of material microstructure. The fabrication of the device using a standard CMOS process – routinely used for analogue and digital circuits – is the key to the sensor's future potential. It allows the associated detection electronics to be constructed on the same piece of silicon as the photodiodes, to form an integrated optical sensor, and work is underway to achieve this. This will significantly reduce much of the complexity, cost and variability of a multi-channel detector system.

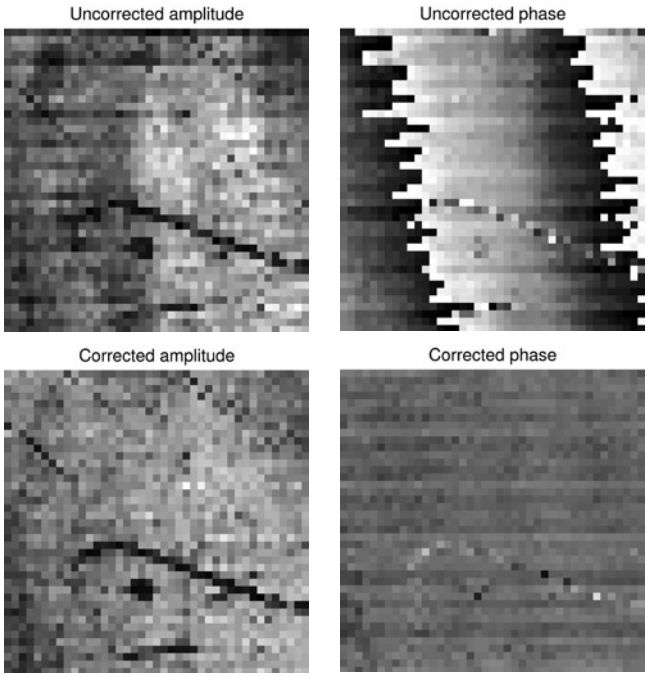

Figure 5. 2 mm x 2 mm amplitude (left) and phase (right) C-scans at 82 MHz on aluminium acquired before (top) and after (bottom) aberration correction

We would like to acknowledge the support of the RCDNE, EPSRC and Rolls-Royce Aeroengines for their continued support.

References

1. R K Tyson, Principles of adaptive optics. Academic Press, 1991.
2. M Clark, S D Sharples, and M Somekh, 'Laser ultrasonic microscopy,' Materials Evaluation, vol 60, no 9, pp 1094–1098, 2002.
3. S D Sharples, M Clark, and M G Somekh, 'All-optical adaptive scanning acoustic microscope,' Ultrasonics, vol 41, no 4, pp 295–299, 2003.
4. M Clark, S D Sharples, and M G Somekh, 'Fast all-optical Rayleigh wave microscope: Imaging on isotropic and anisotropic materials,' IEEE Transactions on Ultrasonics, Ferroelectrics and Frequency Control, vol 47, no 1, pp 65–74, 2000.
5. S D Sharples, M Clark, and M G Somekh, 'Dynamic higher-order correction of acoustic aberration due to material microstructure,' Applied Physics Letters, vol 81, no 12, pp 2288–2290, 2002.
6. J W Goodman, Introduction to Fourier Optics. McGraw-Hill, 1968.
7. S D Sharples, M Clark, and M Somekh, 'Surface acoustic wavefront sensor using custom optics,' Ultrasonics, vol 42, p 647–651, 2004.